Electrochemistry and ESR Spectroscopy of Hemin and Hemeoctapeptide from Equine Cytochrome-*c* with Several Ligands

GEOFFREY J. HAMILTON [1], JOHN W. OWENS

Department of Chemistry, University of New Orleans, New Orleans, La. 70148, U.S.A.

CHARLES J. O'CONNOR* and RICHARD J. KASSNER

Department of Chemistry, University of Illinois at Chicago, Box 4348 Chicago, Ill. 60680, U.S.A.

Received April 2, 1984

Abstract

The cyclic voltammograms and ESR spectra are reported for a series of ligands coordinated to hemin and the ferric hemeoctapeptide (H8PT). The ligands consist of small anions as well as five membered and six membered aromatic and nonaromatic heterocycles with nitrogenous and oxygenous donor atoms. The electrochemistry of the heme-ligand complexes is studied in DMF solution. The axial imidazole coordination from the histidine in H8PT has the effect of attenuating the potential shift caused by the ligand occupying the *trans* axial position.

Introduction

The great variety of processes in which heme proteins participate is due in part to the rather unique physical properties of iron in a porphyrin environment. The literature contains many reports of heme complexes which are described as synthetic models of the various heme proteins [2–8]. The success of model complexes in simulating metalloproteins is evidenced by our increased knowledge of the intricate nature of heme proteins [9–11], much of this knowledge provided by model complexes.

Recently, several groups have reported studies on the ferric heme octapeptide (H8PT) isolated from cytochrome-*c* as a model system for many heme proteins [12–22]. The ferric heme octapeptide is illustrated in Fig. 1. The advantage of this heme protein model is that some of the protein environment is maintained by the presence of peptide, while the molecular size (MW 1500) is much more manageable than that of the native cytochrome *c*.

The peptide portion of the ferric heme octapeptide is covalently linked to the porphyrin ring and is also attached to the iron via the histidine residue with axial imidazole coordination. The remaining axial position of the iron in the H8PT may be occupied by various exogenous ligands. In this work the H8PT and hemin chloride are treated with a series of ligands in order to observe the change in electroactivity and electron structure of the heme unit upon coordination of the axial position(s) by the added ligand. The ligands consist of small anions as well as five and six membered aromatic and non-aromatic heterocycles with nitrogenous and oxygenous donor atoms. The heme-ligand complexes are characterized by cyclic voltammetry and ESR spectroscopy.

CYS-ALA-GLN-CYS-HIS-THR-VAL-GLU

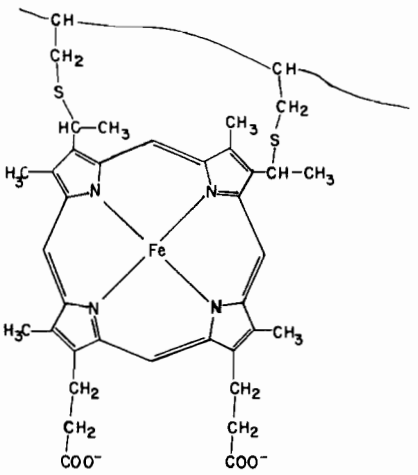

HEME OCTAPEPTIDE

Fig. 1. Diagram of the heme octapeptide unit showing the peptide portion attached to the porphyrin. The histidine residue is bonded to one axial position via the imidazole group.

Experimental

Materials

Spectroscopic grade N,N-dimethylformamide (DMF) was obtained from Matheson, Coleman & Bell

*Author to whom correspondence should be addressed.

0020-1693/84/$3.00

and was fractionally distilled from calcium oxide prior to use. The background electrolyte tetra-n-butylammonium perchlorate (TBAP) was used as supplied by Pfaltz and Bauer Inc. The ligands were used as supplied by the various chemical suppliers, principally Aldrich Chemical Co. Inc. & J. T. Baker Chemical Co. The hemin was obtained from SIGMA Chemicals and recrystallized from DMF. The heme octapeptide was isolated following a published procedure [20].

Electrochemistry

The potential ramp was provided by a P.A.R. 175 Universal Programmer coupled to a P.A.R. 173 Potentiostat which contains a P.A.R. 176 Current-to-Voltage converter. These were used to drive both a Houston Instruments 2000 X-Y recorder and a Tektronix Inc. Type 564B Storage Oscilloscope.

The electrodes were platinum button working electrode, platinum foil auxiliary electrode and either a platinum wire or silver/silver chloride reference electrode in a cell requiring a minimum sample volume of 2 ml. The platinum wire reference electrode was used for convenience and potentials were measured against an internal ferrocene standard [23].

In each case the background electrolyte and solvent were scanned over ±1 V to ensure no residual material from the previous experiment and that there was no contamination of solvent/solute. The ligand was dissolved in the DMF/TBAP solution and tested for electroactivity. If the ligand was electroactive then the region of this activity was noted in order not to assign porphyrin activity to ligand activity. Hemin was then added and after a short period, during which N_2-boil-off from liquid nitrogen was bubbled through the solution, the cyclic voltammogram was recorded.

To check for consistency of the potential measurement both the Ag/AgCl reference electrode and a saturated calomel electrode (SCE) were used to determine E of the Fc/Fc^+ (ferrocene/ferrocenium) couple. E *vs.* SCE = 470 mV (4 measurements), E *vs.* Ag/AgCl = 535 mV (12 measurements), 'ΔE' = 65 mV and compares favorably with the potential of 70 mV directly measured between SCE and Ag/AgCl in 0.1 *M* TBAP in DMF. (In *aqueous KCl*, the expected value is 58 mV).

ESR

The solvent used to prepare the hemin complexes was DMF. The hemin solutions of pyridine (PYR), 4-picoline (4-PIC), quinoline (QUIN), and pyridine-N-oxide (PYR-NO), were prepared by dissolving 0.1 mmol hemin in 3 ml of a solution prepared as a 2:1 ligand/DMF pair. The DMF was used to increase the solubility of the hemin. Complexes of the ligands: azide (N_3^-), imidazole (IM), 4-cyanopyridine (4-CNPYR), and 4-phenylpyridine (4ϕPYR) were prepared by dissolving 0.1 mmol hemin in 3 ml of DMF saturated with the appropriate solid ligand or its sodium salt. The ratio of ligand to heme was greater than 100 in all cases.

The heme octapeptide complexes were prepared by adding 0.05 mmol H8PT to a 1 ml solution of 1:1 ethylene glycol/40 m*M* phosphate buffer (pH = 7.1), saturated with the appropriate ligand.

The ESR measurements were carried out at 77 K, using a Varian-E3 Spectrometer (X-band), equipped with a liquid nitrogen temperature device. Because of the 77 K temperature limitation, and the sizeable spin–lattice relaxation, no signals could be resolved for some low spin complexes. In such cases, literature values for 4 K measurements were substituted, when available.

Results and Discussion

The ESR spectra of hemin/L and H8PT/L complexes where the axial ligand, L, is DMF (solvent), or N_3^- are illustrated in Fig. 2. Table I lists the ESR values for several hemin/ligand and H8PT/ligand complexes along with their assigned spin state configuration. The spectra may be readily interpreted as arising from high spin iron(III) in hemin and H8PT solvent complexes, a mixture of high and low spin iron(III) in hemin/N_3^- and low spin iron(III) in H8PT/N_3^-. The low spin state of iron in H8PT/N_3^- at 77 K is consistent with the ground state assignment based on the observed [22] temperature dependent spin equilibrium of this complex at higher temperatures. In general, the more strongly bonded nitrogenous and CN^- ligands will produce an iron(III) electronic configuration tending toward low spin. The oxygenous ligands will tend to produce high spin ferric heme complexes. The spectra in Fig. 2 and the spin state assignments are very similar to those obtained by Neya and Morishima [24] for the hemin/ligand adducts in DMSO solutions.

Figure 3 illustrates a typical cyclic voltammogram obtained for the hemin/4-picoline complex in DMF solution with 0.1 *M* TBAP supporting electrolyte. Several other types of ligands were tested with hemin in DMF solution and the results of these experiments are summarized in Table II.

Table II also compares the voltages obtained from cyclic voltammetry for the imidazole, pyridine and 4-picoline adducts with hemin measured in a macrocell (2 ml volume) and a microcell (100 μL volume) described in Fig. 4. Data were recorded in both cells to determine the validity of the small volume cell in the electrochemical investigation of the heme octapeptide. Our results indicate that the microcell with the working electrode separated from the other two electrodes by a solvent/electrolyte soaked porous glass gives reliable results.

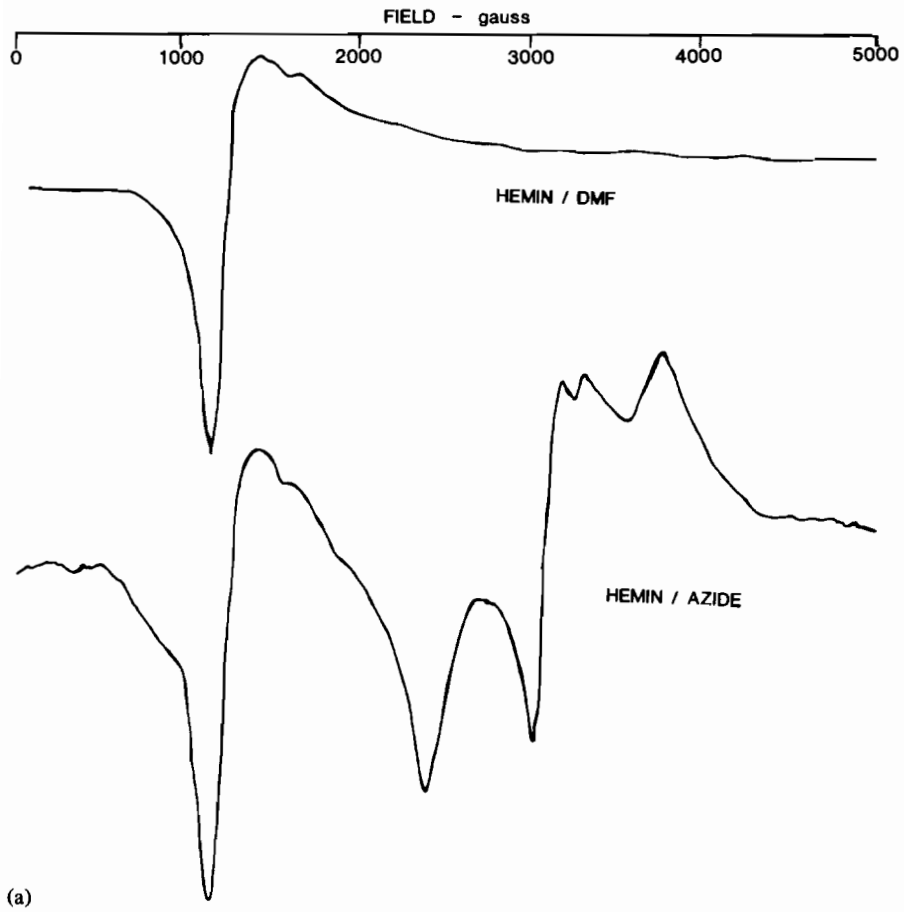

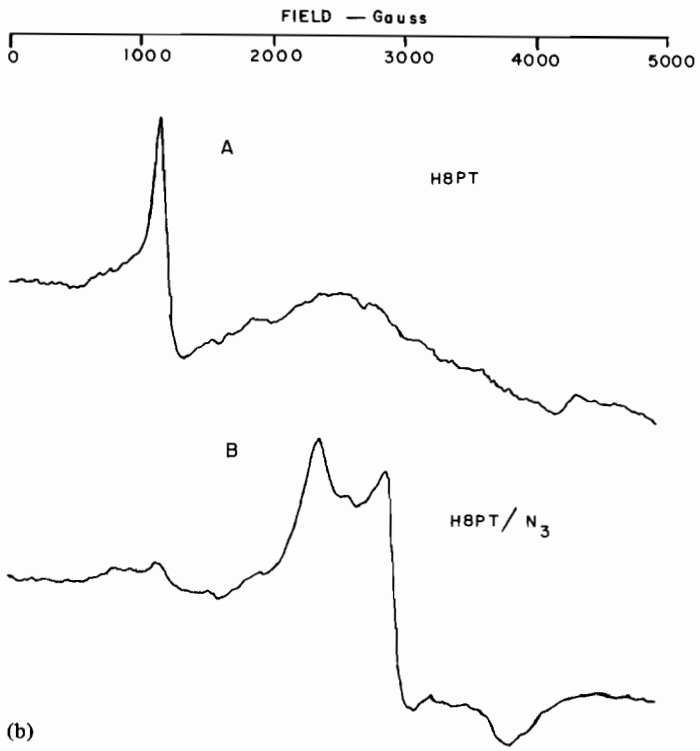

Fig. 2. ESR spectra of hemin ligand adducts in frozen solution at 77 K. a) hemin/L in DMF, b) H8PT/L in ethylene glycol: phosphate buffer solvent. The solutions were prepared as described in text.

TABLE I. ESR Values for Some Low Spin Complexes.

Ligand	Hemin g-value	Spin state	Ref.	H8PT g-value	Spin state	Ref.
DMF	5.91, 2.0	HS	a			
N_3^-	5.27, 280, 2.08, 1.74	HS/LS	a	2.81, 2.14, 1.71	LS	a
CN^-	3.6, 2.3, 1.0	LS	b	3.28, 1.97, 1.16	LS	c
PYR	2.45, 2.15, 1.89	LS	d	3.29, 2.06, 1.70	LS	c
Im	2.96, 2.17, 1.54	LS	a			
4-CN PYR	3.25, 2.25, 1.10	LS	e			
Quinoline	3.48, (others) (unresolved)	LS	e			
4-ϕPYR	3.46, 2.42, 0.81					
4-(picoline)		LS	e			
I^-	6.00, 2.00	HS	f	5.52, 2.17	HS	a
Ethylene glyol/H_2O PO_4 buffer				5.27, 2.06	HS	a

[a]This work. [b]K. Wuthrich, *Struct. Bonding, 8*, 53 (1970). [c]G. McLendon and M. Smith, *J. Am. Chem. Soc., 103*, 4912 (1981). [d]E. von Goldammer, H. Zorn and A. Daniels, *J. Biochem., 57*, 291 (1975). [e]M. Iwainzumi and C. T. Migita, *J. Am. Chem. Soc., 103*, 4378 (1981). [f]Momenteau *et al.*, *Biochim. Biophys. Acta, 320*, 652 (1973). [g]The spectrum indicates a small contribution of LS signal. [h]The spectrum indicates a small contribution of HS signal.

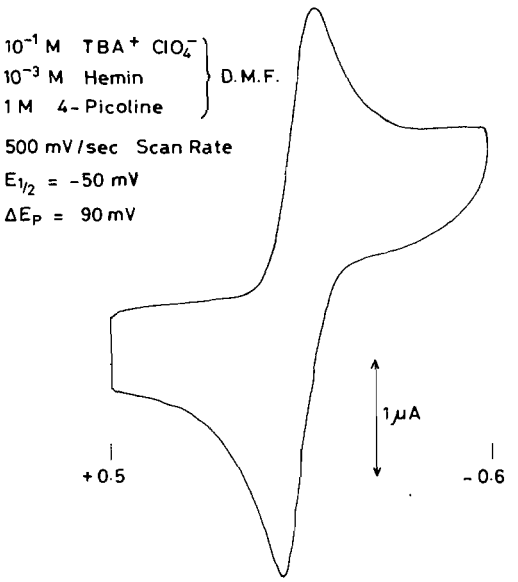

Fig. 3. Cyclic voltammogram trace of hemin 4-picoline adduct. Experimental conditions are indicated in the figure.

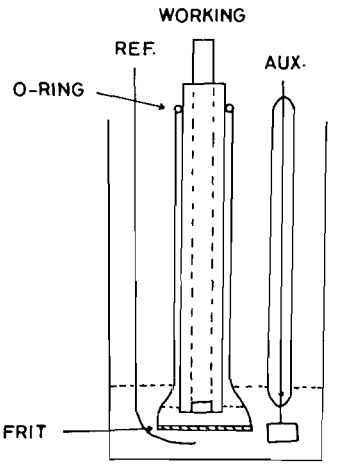

Fig. 4. Schematic diagram of the micro-electrochemical cell used to record cyclic voltammograms of H8PT ligand adducts. This cell allows measurement with sample volumes in the 100 μL range.

Since only small quantities of the heme octapeptide were available, a microcell was required to obtain the cyclic voltammogram (CV) of 100 μL quantities of solution. The reference solution and the microsolution were degassed before measurements were taken. A cyclic voltammogram scan of H8PT: CN^- in DMF using the microcell is shown in Fig. 5. Table III lists the results of the CV measurements for several H8PT ligand adducts using the microcell.

Initially an attempt was made to correlate the $E_{1/2}$ with the pK_a values of all the ligands investigated. This comparison had been done previously for a series of 3- and 4-substituted pyridines and of carboxylic acids and of benzoic acids [25–31]. However, in our study, the ligand changes include not only those from 5 and 6 membered rings containing N and O donor atoms but also steric effects associated with coordination of quinoline and 2-picoline N-oxide.

Observations and generalizations are rather difficult to justify with such a broad range of ligands. However, our data indicate that the more sterically crowded ligands, produce highly asymmetric CV traces which are indicative of a loss of ligand upon reduction of iron(III) to iron(II). Variation in scan width has shown that the widely separated waves are related; *e.g.* with 4-cyanopyridine, the oxidation wave at +230 mV (*vs.* Ag/AgCl) is only achieved if the scan is extended beyond −220 mV (*vs.* Ag/AgCl) at which potential the reduction peak for the complexed hemin appears.

TABLE II. Representative Data for Hemin $(L)_2$ *vs.* F_c^+/F_c.

Ligand	pK_a	$\Delta E_{1/2}$ (mV)	Comments
Imidazole	6.95	−730	'Macrocell'
		−715	'Microcell'
Pyridine	5.25	−435	'Macrocell'
		−435	'Microcell'
4-Picoline	6.02	−450	
Morpholine	8.33	−770	
Pyridine-N-oxide	0.79	−790	
4-Picoline-N-oxide	1.29	−750	

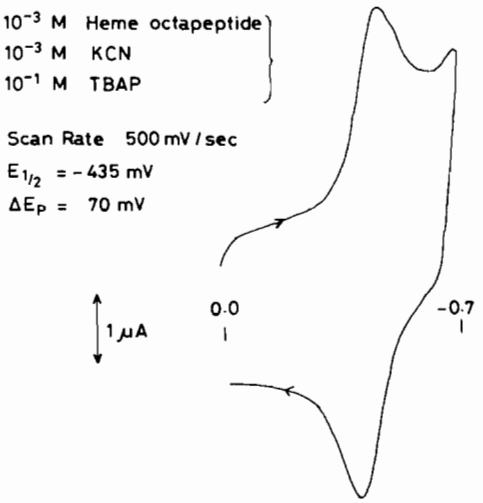

Fig. 5. Cyclic voltammogram trace of H8PT ligand adduct. Experimental conditions are described in the figure.

TABLE III. Data for Hemeoctapeptide (L) *vs.* F_c^+/F_c.

Ligand	pK_a	$\Delta E_{1/2}$ (mV)
Imidazole	6.95	−765
Pyridine	5.25	−660
Morpholine	8.33	−770
2-Picoline-N-oxide		−715
Pyridine-N-oxide	0.79	−740

Scan rates up to 100 V/sec indicate little or no change in both reduction and oxidation potentials. This means that any rearrangement of the iron(II) coordination sphere is faster than our instrumentation will reasonably observe. If rearrangement were in the range available, two peaks might be expected on the oxidation scan and the peak resulting from the rearranged iron(II) coordination sphere would be expected to decrease with increasing scan rate.

Since there is a change in electronic structure and spin state as the coordination ligand is varied for heme systems, we had hoped to investigate the resultant electrochemical effects of this phenomena. However, a correlation between the reduction potential of the Fe^{III}/Fe^{II} couple and the spin state of the iron species has not been observed in the data obtained by Kadish and co-workers [32–39] on some other heme and non-heme iron complexes.

An interesting correlation is evident when the reduction potentials of hemin/L are compared with H8PT/L for the series of ligands studied. The effect of the ligand on the value of the reduction potential is attenuated in the H8PT/L adduct when compared to the hemin/L adduct. The range of $\Delta E_{1/2}$ potentials (relative to the ferrocene internal standard) spanned by the hemin/adducts is from $\Delta E_{1/2} = -345$ mV for the pyridine adduct to $\Delta E_{1/2} = -790$ mV for the pyridine N-oxide adduct. This is a range of a little more than 350 mV. The potential difference of 295 mV between the imidazole and pyridine complexes of hemin may be compared to a difference of 316 mV between the hystidyl imidazole [7] and pyridine [40] complexes of mesoheme [41]. The potentials spanned by the H8PT/L adducts is from $\Delta E_{1/2} = -660$ mV for the pyridine adduct to $\Delta E_{1/2} = -770$ mV for the morpholine adduct, or a range of only 110 mV. The potential difference of 105 mV between the imidazole and pyridine complexes of H8PT is consistent with a difference of 102 mV between the imidazole [13] and pyridine [42] complexes of the heme undecapeptide from cytochrome *c* in aqueous solution at 30 °C.

It is interesting to note that in addition to attenuating the voltage shift due to the ligand, the $\Delta E_{1/2}$ values are shifted toward the value measured for hemin/imidazole. It therefore appears that the coordination of the histidyl imidazole group in the H8PT has a stabilizing effect on the reduction potential of the iron heme system. This effect may be important for the finely controlled voltages that occur in the cytochrome respiratory cycle.

Acknowledgements

This investigation was supported in part by grants from the National Institute of Health (AM28188 and HL26216) to R. J. K. and the Graduate Research Council of The University of New Orleans to C. J. O.

References

1 On sabbatical leave from the Footscray Institute of Technology, Melbourne, Australia.
2 J. P. Collman, *Acc. Chem. Res., 10*, 265 (1977). J. A. Ibers and R. H. Holm, *Science, 204*, 233 (1980).
3 T. Hashimoto, R. L. Dyer, M. J. Crossley, J. E. Baldwin and F. Bosolo, *J. Am. Chem. Soc., 104*, 2101 (1982).
4 D. M. Collins, R. Countryman and J. L. Hoard, *J. Am. Chem. Soc., 94*, 2066 (1972).
5 L. J. Radonovich, A. Bloom and J. L. Hoard, *J. Am.*

Chem. Soc., 94, 2073 (1972).
6 W. R. Scheidt, I. A. Cohen and M. E. Kastner, *Biochemistry, 18*, 3546 (1979).
7 P. K. Warme and L. P. Hager, *Biochemistry, 9*, 1606 (1970).
8 D. H. Dolphin, J. R. Sams and T. B. Tsin, *Inorg. Chem., 16*, 711 (A77).
9 M. F. Perutz, *Brit. Med. Bull., 32*, 193 (1976).
10 E. Antonini and M. Brunori, 'Hemoglobin and Myoglobin in Their Reactions with Ligands', Elsevier, New York, N.Y., 1971.
11 J. L. Hoard in 'Porphyrins and Metalloporphyrins', K. M. Smith, Ed., Elsevier, Amsterdam, 1975, Chapter 8.
12 J. Peterson, J. Silver, M. T. Wilson and I. E. G. Morrison, *J. Inorg. Biochem., 13*, 75 (1980).
13 H. A. Harbury and Paul A. Loach, *J. Biol. Chem., 235*, 3640 (1960).
14 H. Harbury and Y. P. Meyer, *Ann. N.Y. Acad. Sci.*, 685 (1966).
15 M. Smith and G. J. McLendon, *J. Am. Chem. Soc., 102*, 5666 (1980).
16 M. Smith and G. McLendon, *J. Am. Chem. Soc., 103*, 4912 (1981).
17 G. McLendon and M. Smith, *Inorg. Chem., 21*, 847 (1982).
18 D. C. Blumenthal and R. J. Kassner, *J. Biol. Chem., 255*, 5859 (1980).
19 D. C. Blumenthal and R. J. Kassner, *J. Biol. Chem., 254*, 9617 (1979).
20 Y. Huang and R. J. Kassner, *J. Am. Chem. Soc., 103*, 4927 (1981).
21 Y. Huang and R. J. Kassner, *J. Biol. Chem., 256*, 5327 (1981).
22 Y. Huang and R. J. Kassner, *J. Am. Chem. Soc., 101*, 5807 (1979).
23 R. R. Gagne, C. A. Koval and G. C. Lisensky, *Inorg. Chem., 19*, 2854 (1980).
24 S. Neya and I. Maristima, *J. Am. Chem. Soc., 104*, 5658 (1982).
25 D. G. Davis, 'The Porphyrins', Vol. V, D. Dolphin, Ed., Academic Press, New York (1978) p. 127.
26 R. Cheng, L. Latos-Grazynoki and A. L. Bach, *Inorg. Chem., 21*, 2412 (1982).
27 P. Bianco and J. Haladjian, *J. Electroanal. Chem., 137*, 367 (1982).
28 M. J. Richard, C. D. Shaeffer and R. F. Evilia, *Electrochim. Acta, 27*, 979 (1982).
29 S. Ni, L. Dickens, J. Toppan, L. Constant and D. G. Davis, *Inorg. Chem., 17*, 228 (1978).
30 L. Constant and D. G. Davis, *J. Electroanal. Chem., 74*, 85 (1976).
31 K. M. Kadish, M. M. Morrison, L. A. Constant, L. Dickens and D. G. Davis, *J. Am. Chem. Soc., 98*, 8387 (1976).
32 K. M. Kadish, C. H. Su and L. J. Wilson, *Inorg. Chem., 21*, 2312 (1982).
33 L. A. Bottomley and K. M. Kadish, *Anal. Chim. Acta, 139*, 367 (1982).
34 L. A. Bottomley and K. M. Kadish, *Inorg. Chem., 20*, 1348 (1981).
35 R. H. Petty, B. R. Welch, L. J. Wilson, L. A. Bottomley and K. M. Kadish, *J. Am. Chem. Soc., 102*, 611 (1980).
36 K. M. Kadish and L. A. Bottomley, *Inorg. Chem., 14*, 832 (1980).
37 K. M. Kadish, K. Das, D. Schaeper, C. L. Merrill, B. R. Welch and L. J. Wilson, *Inorg. Chem., 19*, 2816 (1980).
38 K. Kadish, G. Larson, D. Lexa and M. Momenteau, *J. Am. Chem. Soc., 97*, 282 (1975).
39 B. A. Feinberg, M. Gross, K. M. Kadish, S. J. Pace and J. Jordan, *Bioelectrochem. Bioenergy, 1*, 73 (1974).
40 T. H. Davies, *J. Biol. Chem., 135*, 597 (1940).
41 R. J. Kassner, *Proc. Nat. Acad. Sci., U.S.A., 69*, 2263 (1972).
42 H. A. Harbury and P. A. Loach, *J. Biol. Chem., 235*, 3646 (1960).